



# The Effect of Irregularity of Lateral Stiffness in Estimating the Separation Gap of Adjacent Frames

Mostafa Khatami<sup>1a</sup>, Mohsen Gerami<sup>2b</sup>, Ali Kheyroddin<sup>2b</sup>, and Navid Siahpolo<sup>3c</sup>

<sup>a</sup>Structural Engineering, Semnan University, Semnan 35131-19111, Iran

<sup>b</sup>Faculty of Civil Engineering, Semnan University, Semnan 35131-19111, Iran

<sup>c</sup>Dept. of Civil Engineering, Academic Center of Education-Culture-Research, Khouzestan Branch, Ahwaz 84689-61396, Iran

## ARTICLE HISTORY

Received 26 January 2019  
Revised 24 August 2019  
Accepted 1 November 2019  
Published Online 9 December 2019

## KEYWORDS

Normalized separation gap  
Collision level  
Irregularity factor  
Adjacent buildings  
Nonlinear viscoelastic element

## ABSTRACT

Structural pounding can lead to local or total damage to the stories at the collision level or to the overall collapse of the building. On the other hand, lateral stiffness irregularity is common in the form of soft or very soft stories, which is due to the alternation in the type of function of the first story of the building. This paper estimates the demand for the normalized separation gap (NSG) at adjacent buildings' highest collision level that were a combination of regular and irregular frames. For this purpose, the steel moment resisting frames (MRF), compounds with a total of 700 adjacent states and their NSG, is calculated by the dynamic time history analysis. In addition, irregularity increment in lateral stiffness for the first story could lead to an increase in the NSG of 84% of the adjacent combinations. In this study, a new relationship is proposed to estimate the demand for the NSG with the consideration of the effects of irregularity of lateral stiffness in the lowest story.

## 1. Introduction

Pounding was a phenomenon that occurred due to the collision of two structures, with overall or partial destruction of the structures caused by lateral forces. Actually, when pounding occurred, a large force was imposed on the structure in a short time, which had not been considered in common designs. In large cities and in densely populated areas, landowners did not desire to be distanced between buildings due to land costs. Therefore, during an earthquake, the two buildings would get lateral displacements considering the dynamic characteristics. Most of these displacements occurred between them in an uneven phase mode, because of the difference in this specification. These uneven-phase displacements between the two buildings lead to their pounding. This phenomenon had been observed in most of the world's large-scale earthquakes (Kheyroddin et al., 2018; Karayannis and Favvata, 2005; López and Kharazian, 2018; Shehata and Raheem, 2014).

Various approaches had been proposed, including the use of interface elements between the two structures in order to integrate their responses, the use of flexible materials between structures,

and the use of response reducing equipment such as dampers to reduce seismic demand.

One of the factors, that could prevent pounding largely, was embedding the separation gap between the buildings. Several studies have been conducted to calculate required separation gap, to avoid adjacent frames collision. The research of Shrestha (2013) showed that summation of absolute displacements (ABS) and square root of summation of squares of displacements (SRSS) overestimated the amount of separation required in the linear and nonlinear structures, especially when the two structures had the same periodicity (similar dynamic characteristics). The values of the spectral difference method (DDC), especially in the domain of structures with equal period values, were in good agreement with the analytical results (Shrestha, 2013). Pounding of irregular adjacent buildings at a height (with the setback) was examined by Efraimiadou et al. (2013a). The results showed the lateral displacement of the time history analysis and the separation gap depended on the layout of the adjacent frames and the rate of irregularity. In addition, by scoring various adjacent combinations based on the different seismic demands, it was concluded that the conditions became

**CORRESPONDENCE** Mohsen Gerami ✉ mgerami@semnan.ac.ir 📧 Faculty of Civil Engineering, Semnan University, Semnan 35131-19111, Iran

© 2019 Korean Society of Civil Engineers

more critical by increasing the height of the collision of two structures (Efraimiadou et al., 2013a). In the second part of the research by Efraimiadou et al. (2013b), the pounding in irregular adjacent buildings under seismic sequence was investigated. The results showed that sequencing of earthquake records led to lateral displacement increments for stories relative to the state of the singular earthquake, which resulted in an increment in the separation gap. Moreover, the way of positioning of irregular frames at height next to each other was effective on stories lateral displacements (Efraimiadou et al., 2013b). Hao (2015) examined non-uniform earthquakes' effects on building supports in order to the propagation of waves into the soil and its dependence on soil type and then, the comparison of this type of earthquake with a uniform earthquake. The effect of soil type had also been used in evaluating the results. Major results were in following: the greatest effect of a non-uniform earthquake on the separation gap was when structures had similar vibrational frequencies; its effect was negligible out of the mentioned range. Thus, the separation gap demand would be underestimated if the effects of non-uniform earthquakes were ignored. In addition, by increasing the degree of soil softness, the required separation gap for the two structures increased, due to the larger displacement of the earth (Hao, 2015). Naderpour et al. (2017) proposed a relation for the separation gap via the artificial neural network, based on maximum lateral displacements and the periodic times of the structures. Thus the separation gap would be estimated between structures with different periodic times and high precision (Naderpour et al., 2017). Favvata (2017) studied the required distance in the collision of adjacent RC frames on three seismic hazard levels for different first story levels. Minimum distance results was considered in order to minimize the shear demand for a column or the complete avoidance of collisions between two structures depending on limit state and the seismic hazard level (Favvata, 2017).

According to few conducted studies based on the effects of separation gap irregularities for the adjacent structures, the purpose of this study was to estimate the demand for the NSG of the binary combinations of regular and irregular adjacent steel MRFs. Therefore, for this purpose, this demand was estimated by examining the effect of irregularity of lateral stiffness with variation in the first story height of the frames (due to the change in the type of occupancy).

## 2. Modeling of Collision Element

Lower values of separation gap, result in the collision of adjacent structures, as maximum relative displacement of adjacent buildings exceeded the predicted separation gap demand. For dynamic time history analysis in this study, collision behavior was modeled using the nonlinear viscoelastic elements which was proposed by Jankowski, with collision force calculations as follow (Jankowski, 2005):

$$F(t) = 0 \quad \text{if} \quad \delta(t) \leq 0 \quad (1)$$

$$F(t) = \beta \cdot \delta^{\frac{3}{2}}(t) \quad \text{if} \quad \delta(t) > 0, \dot{\delta}(t) \leq 0 \quad (2)$$

$$F(t) = \beta \cdot \delta^{\frac{3}{2}}(t) + c(t) \cdot \dot{\delta}(t) \quad \text{if} \quad \delta(t) > 0, \dot{\delta}(t) > 0 \quad (3)$$

$$\delta(t) = u_1 - u_2 - g_p \quad (4)$$

$$\dot{\delta}(t) = \dot{u}_1 - \dot{u}_2 \quad (5)$$

In Eqs. (1) to (3),  $g_p$  indicated the separation gap of two adjacent structures. In Eqs. (4) and (5),  $u_1$  and  $u_2$  indicated the lateral displacements of the two adjacent structures. Calculating the collision force for different separation gaps between the two structures, and approaching the amount of collision force to the value of zero, the minimum separation gap would be provided. In Eqs. (1) to (3),  $\beta$  indicated the collision element stiffness, which was calculated by Eq. (6):

$$\beta = \frac{4}{3\pi(h_1 + h_2)} \sqrt{\frac{R_1 \cdot R_2}{R_1 + R_2}} \quad (6)$$

$$R_i = \sqrt{\frac{3m_i}{4\pi\rho_i}} \quad (7)$$

$$h_i = \frac{1 - \gamma_i^2}{\pi \cdot E_i} \quad (8)$$

In Eqs. (6) to (8),  $\rho_i$ ,  $g_i$ ,  $E_i$ ,  $m_i$  indicated density, Poisson's ratio, modulus of elasticity and mass, respectively.  $R_i$  indicated radius of the collision objects (the floors). Material specification values for ST37 steel were used with modulus of elasticity of  $2.1 \times 10^6$  kg/cm<sup>2</sup>, density of 7,850 kg/m<sup>3</sup>, Poisson's ratio of 0.3. Collision element damping in Eqs. (1) to (3), was calculated from Eqs. (9) and (10):

$$c(t) = 2\xi \sqrt{\beta \cdot \sqrt{\delta(t)} \cdot \frac{m_1 \cdot m_2}{m_1 + m_2}} \quad (9)$$

$$\xi = \frac{9\sqrt{5}}{2} \cdot \frac{1 - e^2}{e(e(9\pi - 16) + 16)} \quad (10)$$

In Eq. (10)  $e$  was the compensation coefficient, with values in range  $0 \leq e \leq 1$  which was based on the experimental studies calculated by Jankowski for steel-to-steel collision considering relative velocity before the collision using Eq. (11) (Vaseghi and Jalali, 2013):

$$e = -0.0039v^3 + 0.0044v^2 - 0.1867v + 0.7299 \quad (11)$$

Equations (1) to (3) showed nonlinear behavior of viscoelastic pounding element which can be modeled as a new material in OPENSEES software. Relations were coded in Visual C++ programming language and OPENSEES source code was compiled. Then the new material was used in the model using TCL programming interpreter. The pounding force effective parameters such as stiffness, damping, and compensation coefficient were

updated in each step, using values of displacement and velocity of the pounding DOFs (Khatami et al., 2019).

### 3. Defining of Studied Frames

The analyzed models had been considered in the form of two-dimensional steel MRFs with high ductility of buildings and numbers of stories: 2, 4, 6, 8, 10, 12, 14, 16, 18 and 20. It worth to note, each frame had three spans. In this study, stories' height in regular frames were constant equal to 3.5m and length of the spans to 5.5 m. For the creation of lateral stiffness irregularity of the first story, the height of this story in the irregular models was considered as 4.5 and 5.5 m, which was classified as very soft story, according to Iranian seismic code (Standard No. 2800, 2014). The 30 frames with and without irregularities had been modelled under gravity and seismic loading based on the 6th Iranian national building code (INBC-No. 6, 2014) and Iranian seismic code (Standard No. 2800, 2014). Distributed values of 650 kg/m<sup>2</sup> and 250 kg/m<sup>2</sup> were determined for floor dead and live loads with 5 m span width. Mass values for all stories had been assumed to be identical. Soil Type III was considered for the construction site, the region considered to be at high risk of earthquake and the occupancy type to be residential property with an average degree of importance.

The equivalent-static analysis and load and resistance factor methods were used to analyze and design all frames using ETABS software (ETABS, 2015), based on Iranian national building code (INBC-No. 10, 2014). Spectral dynamic analysis was performed in some models with and without irregularities, according to Iranian seismic code (Standard No. 2800, 2014). In the design, regardless of the modeling of the panel zone, the

interaction between the soil and structure, and the infilled-frame effects, the roof was considered to be rigid with P-Δ effects. Six types of plate girder were considered for beams including TW300F150TH15 to TW550F250TH20 (which W was web height, F was flange width and TH was the thickness of flange and web in mm), and seven types of box sections for columns including BO × 200 × 15 mm to BO × 500 × 40 mm. Seismic compact sections criteria was considered for all sections. About irregular frames, the design was performed in order to create an irregularity of lateral stiffness according to Standard 2800. Therefore, the height of the first story increased to 4.5 m or 5.5 m, and the same column section was chosen for on the first two stories (stiffness of the frame is changed by variation in the height of the stories). As an example, design results of beams and columns in 4-story regular and irregular frames was presented in Fig. 1. It should be noted that in irregular frames with changing the height of the first story, the frames were analyzed and designed again.

Frames adjacent arrangements were classified in seven groups as shown in Table 1, in two-component combinations, with special priority of the arrangements. Each group represented 100 different arrangement ways of the frames adjacent to each other. Generally, investigations were performed in 700 different adjacent cases and their results had been explained. In the latter table, R was an abbreviation for the regular frames and irregularity factor (I) was defined as ratio of first story's height to other stories' height. Irregularity factor had the values of 1.3 for 4.5 m and 1.6 for 5.5m for first story's height, respectively. The star symbol (\*) indicated the number of examined frame stories, which could range from 2 to 20. For instance, the combination of 2R.4I(1.3) represented for regular 2-story frame on the left side, adjacent to

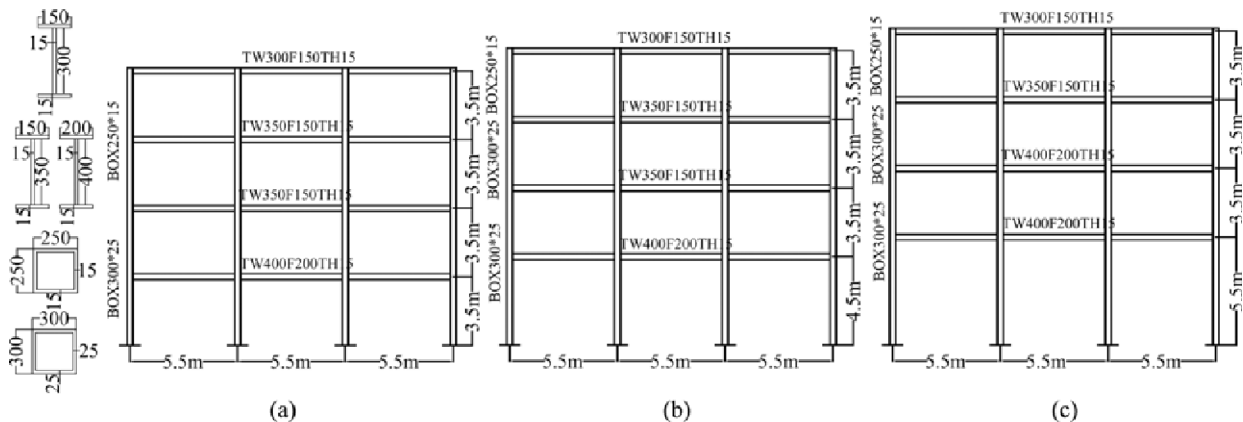
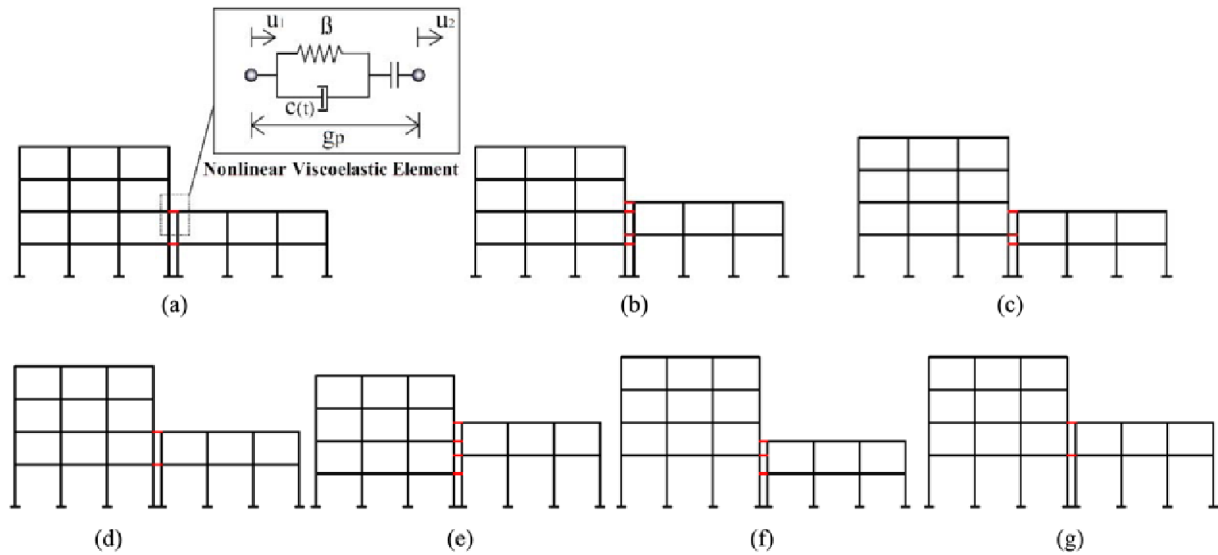


Fig. 1. Results of Designing 4-Story Regular and Irregular Frames in ETABS Software: (a) Dimensions of Sections: mm Frame 4R, (b) Frame 4I (1.3), (c) Frame 4I (1.6)

Table 1. Combinations of Examined Adjacent Frames

Regular basic combination	Irregular combination (with an increment in height of the first story to 4.5 m)			Irregular combination (with an increment in height of the first story to 5.5 m)		
Group 1	Group 2	Group 3	Group 4	Group 5	Group 6	Group 7
*R.*R	*R.*I(1.3)	*I(1.3).*R	*I(1.3).*I(1.3)	*R.*I(1.6)	*I(1.6).*R	*I(1.6).*I(1.6)



**Fig. 2.** Different Adjacent Combinations of 2 and 4-Story as Grouped in Table 1 in OPENSEES Software: (a) 4R.2R, (b) 4R.2I(1.3), (c) 4I(1.3).2R, (d) 4I(1.3).2I(1.3), (e) 4R.2I(1.6), (f) 4I(1.6).2R, (g) 4I(1.6).2I(1.6)

4-story irregular frame with a height of 4.5 m in first story on the right side, for group 2 in Table 1.

Figure 2 showed various combinations of adjacent frames, according to Table 1 which had 2 and 4 stories with nonlinear viscoelastic collision elements between them.

Nonlinear responses of structures including pounding effects were determined by dynamic time-history analyses using OPENSEES (McKenna and Fenves, 2007). Displacement-based

fibers were used for modeling beams. Uniaxial bilinear elastoplastic stress-strain cyclic behavior was considered for each fiber. Steel01 material was used for steel, with a 0.03 hardening ratio. Cyclic degradation was ignored and a rigid elastic behavior was considered for panel zones. Force-based fiber elements were used for modelling columns due to the interaction effects of axial and moment forces. Floors nodes were constrained with axial rigidity, for composite slab diaphragms. Corotational coordinate

**Table 2.** Specifications of 20 Near-Fault Earthquake Records (perpendicular components to the fault)

Number	Earthquake name	Year	Station	PGA(g)	Mw	R(km)	Tp(s)
1	Imperial Valley-06	1979	El-Centro Array#4	0.61	6.53	7.05	4.61
2	Northridge-01	1994	Newhall-Fire Sta	0.18	6.69	5.92	1.03
3	Northridge-01	1994	Newhall-W Pico Canyon Rd.	0.33	6.69	5.48	2.40
4	Northridge-01	1994	Rinaldi Receiving Sta	0.08	6.69	6.50	1.23
5	Northridge-01	1994	Sylmar-Converter Sta East	0.58	6.69	5.19	3.52
6	Kobe, Japan	1995	KJMA	1.05	6.90	0.96	0.95
7	Kobe, Japan	1995	Takarazuka	0.94	6.90	0.27	1.42
8	Landers	1992	Yermo Fire Station	0.10	7.28	23.62	7.50
9	Imperial Valley-06	1979	El-Centro Array#6	0.65	6.53	1.35	3.83
10	Northridge-01	1994	Jensen Filter Plant	0.12	6.69	5.43	3.52
11	Imperial Valley-06	1979	EC Country Center FF	0.32	6.53	7.31	4.51
12	Imperial Valley-06	1979	EC Meloland Overpass FF	0.44	6.53	0.07	3.34
13	Morgan Hill	1984	Coyote Lake Dam(SW Abut)	0.23	6.19	0.53	0.95
14	Loma Prieta	1989	Gilroy - Gavilan Coll	0.25	6.93	9.96	1.79
15	Loma Prieta	1989	LGPC	0.84	6.93	3.88	4.39
16	Northridge	1994	Westmoreland	0.40	6.70	29.00	0.30
17	Northridge-01	1994	Jensen Filter Plant Generator	0.12	6.69	5.43	3.52
18	Northridge-01	1994	Sylmar-Converter Sta	0.65	6.69	5.35	3.47
19	Northridge-01	1994	Sylmar-Olive View Med FF	0.45	6.69	5.30	3.10
20	Kocaeli, Turkey	1999	Gebze	0.30	7.51	10.92	5.78

Mw: Moment Magnitude PGA: Peak Ground Acceleration

R: Closest distance from the ruptured area to recording site Tp: Predominant Period

transformations were set to consider P-Δ effects of the gravity loads in the steel MRF plan. Equations of motion of the steel MRFs subjected to earthquake ground motions were integrated by constant acceleration Newmark method. Unbalanced forces were minimized by tangent stiffness Newton method in each integration time step. A dynamic programming technique was used to decrease time step value to overcome convergence issues, whenever this decrement was needed. Rayleigh damping matrix was calculated with the inherent damping ratio of 5% at the first two modes of vibration. To avoid large damping forces, nonlinear springs were modeled with high initial stiffness values in proportional pounding DOFs (Khatami et al., 2019).

### 4. Earthquake Records

Near-fault pulse-shape records were used on soil type III, for nonlinear dynamic analyses of 20 perpendicular components for a progressive orientation fault. These records were taken from Pacific Earthquake Engineering Research Center (PEER, 2018) and had been classified by Baker (Baker, 2007). Dominant pulse period of the velocity was considered in choosing accelerograms, to be in the range of fundamental periods for the studied frames. For all selected records, an interval of 0.005s had been used. Earthquake records were uniformly applied and the effects of variations were not considered in the distance from the source. Accelerogram specifications were shown in Table 2.

Time history accelerograms were scaled according to Iranian Standard using Seismosignal software (SeismoSignal, 2016). The scale factors for the period range of the studied frames from 0.55 to 0.85 were extracted.

### 5. Modeling Verification

In order to verify the accuracy of the results, an experimental reference model (Takabatake et al., 2014) was chosen with two single span frames and four stories, placed on one-directional shaking table in the laboratory, as shown in Fig. 3(a). The span, height and depth of the frames were 0.2 m, 0.6 m and 0.15 m,

respectively. All the stories were considered to be 0.15 m height. Additional masses of 6.5 Kg in all stories was used in frame F-A. The dimensions of the frame columns were 0.03 m × 0.0016 m from the SS400 iron and the columns resisted against bending around the weak axis in the vibration direction. The frames floors was made up of aluminum rectangular plates with 0.15 m × 0.2 m × 0.015 m dimensions, with no beams. The separation gap at the highest level of two frames had been considered to be 2 mm. EL-Centro 1940 NS earthquake was normalized to 0.5 m/s maximum velocity and applied to the shaking table. The collision force at the highest level had been measured by strain gauges installed at the top and bottom of the junction.

The analytical model consisted of two frames with 4-DOFs with concentrated masses in the roof levels based on the reference model (Takabatake et al., 2014) analyzed in OPENSEES. Damping coefficient of 0.02 was determined for each frame. As proposed by Jankowski, a nonlinear viscoelastic collision element had been used for the modeling of pounding. The coefficient of compensation was assumed to be 0.63. The experimental and analytical collision result forces were compared based on the ELCN record, with 2 mm separation gap. The form of variations and maximum collision forces at the highest level were shown in Fig. 3(b) with acceptable consistency, showing the maximum pounding forces of analytical and experimental models to be 67.30 KN and 61.50 KN, respectively.

To verify the accuracy of the separation gap results achieved with the behavior of this element, the results of the separation gap were compared with the values obtained from the lateral displacement difference at the highest level of collision. In the recent case, the separation gap had been extracted from the investigation of six possible modes for the aim of preventing collisions of two structures based on the dynamic displacement differences of adjacent MRFs during the analysis. As an example, Fig. 4(a) showed lateral displacement time history for 2 and 4-story MRFs under record No. 9. Based on the amount and direction of the corresponding lateral displacement of these two frames during the analysis, the time history of the separation gap for the 2-story frame was, as shown in Fig. 4(b), on the left side

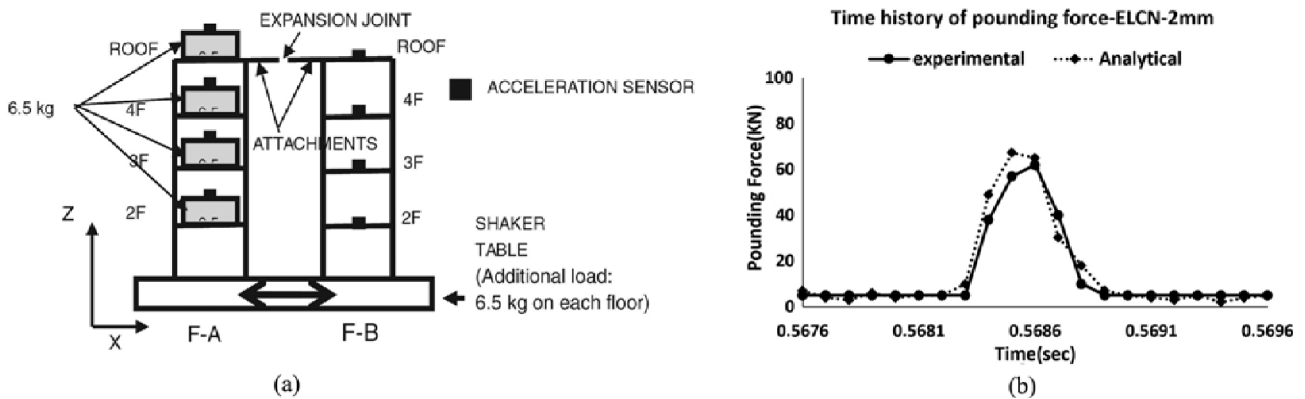


Fig. 3. Experimental Sample Details and Time History of the Collision Force in Experimental and Analytical Models: (a) Schematic Diagram of Pounding Test (Takabatake et al., 2014), (b) Separation Gap of 2 mm

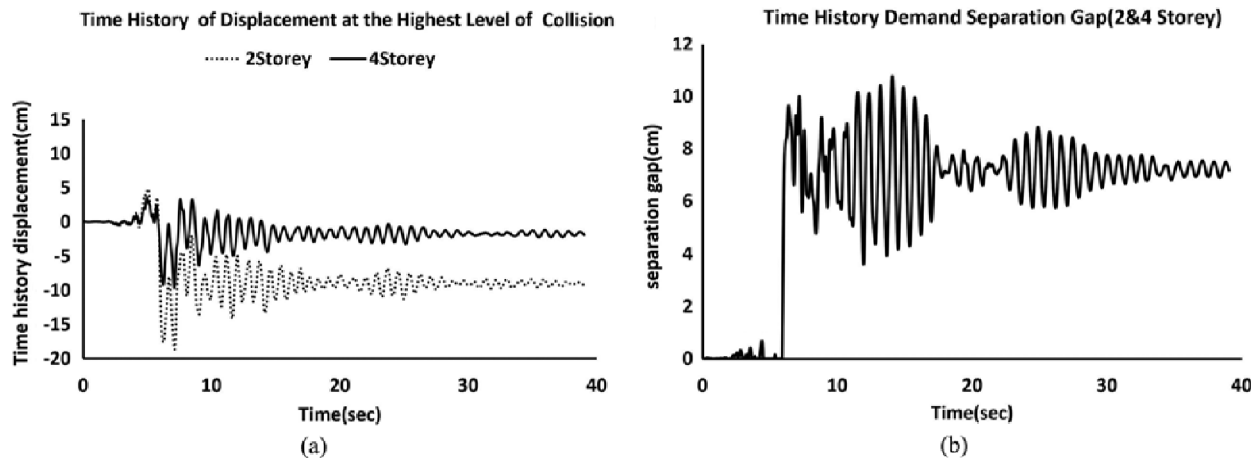


Fig. 4. Lateral Displacement Time History and Separation Gap of 2 and 4-Story Regular Frames with: (a) Lateral Displacement under Record No. 9, (b) Separation Gap under Record No. 9

and for the 4-story frame was on the right side of the adjacencies. As shown in Fig. 4(b), the maximum required separation gap of these two structures under the record of No 9 was 10.7 cm. The value of the separation gap of the collision element modeling method for this record was 11.1 cm, and the values obtained from the two methods had acceptable adaptation.

## 6. Results of Dynamic Time History Analysis

Comparing the results of the dynamic time history analysis and regulations on NSG, the effects of lateral stiffness irregularities on NSG was also investigated. Non-dimensional NSG was defined as the required separation gap divided by the collision height of two frames at the highest collision level. In addition, the experimental relationships presented in Standard 2800 had been used to obtain the ratio of the fundamental period of the sway of two adjacent frames.

### 6.1 Comparison of the Results of Dynamic Time History Analysis and Building Regulation in Regular Frames

The average difference of the NSG obtained from dynamic analysis and the criteria of Iranian seismic code under 20 perpendicular components to the near-fault for different combinations of placement of the 8-story buildings, or the building with lower stories, in vicinity of each other was compared in Fig. 5. In this figure, the horizontal axis was the ratio of the period of the various frames on the right side of the basic 2-8-story frame on the left side and the criterion of section 1.4.1 had been used to calculate the NSG according to the Standard 2800 for buildings up to eight stories. According to this section, the distance between each story and the adjacent land boundary would be at least equal to 0.005 of that story height from the base.

The results showed that as the period of the two structures approached to each other, the difference between the analytical and the regulation values would reach to the maximum amount. The reason for this is that, in analytical terms, two adjacent frames with identical period values and similar dynamic properties

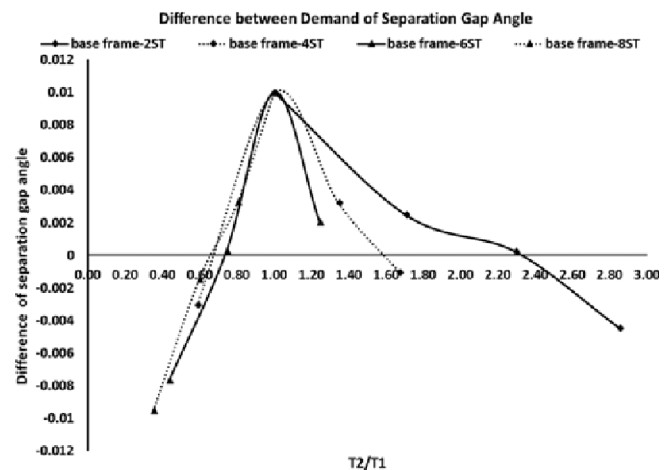


Fig. 5. Difference in the Demand of NSG in the Analytical and Regulation Results Based on Section 1.4.1 of the Standard 2800

did not require separation gap. In cases, which this difference was negative (the angle difference of the separation gap was less than zero), the analytical results exceeded the values of section 1.4.1 of the Standard 2800 which represented the underestimation of the angle of separation gap based on building regulation. In the ratio of the period, which was less than 1, this difference relative to the height of base frame had no certain trend; but, in the ratios of the period, which was more than 1, by increasing the height of the base frame, the difference between the analytical and regulation values was reduced for a given period ratio.

The average difference between the NSG obtained from the dynamic time history analysis and Standard 2800 (ASCE/SEI 7-16, 2016) was compared under the 20 perpendicular components to the near-fault based on different combinations of placement of the buildings, which had more than eight stories adjacent to each other in Fig. 6. In this figure, the horizontal axis was the period ratio of the various frames on the right side to the base frame

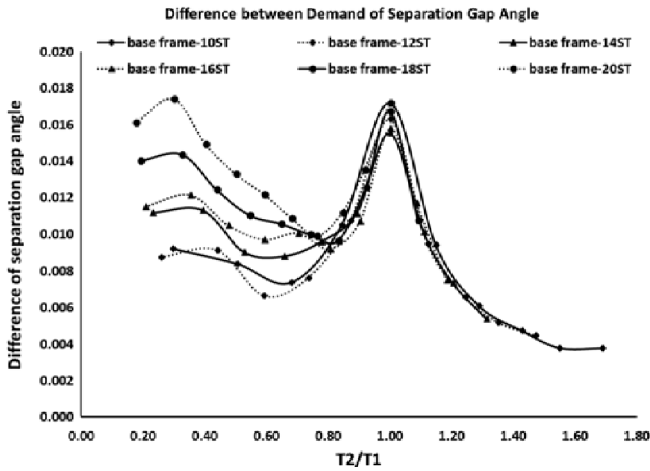


Fig. 6. Difference between the Separation Gap Values of the Analysis and the Regulation in Section 6.5.3 of Standard 2800

with 10 to 20-story on the left side. Regulations of section 6.5.3 had been used to calculate the NSG (section 12.12.3 of the ASCE7-16), according to this paragraph, the SRSS method of nonlinear lateral displacements had been proposed to calculate the structures' separation gap.

As shown in Fig. 6, period ratio increment (right frame to left frame) generally led to decrement of the difference between the results of the analysis and Iranian seismic code criteria, except in the same range of periods, which difference of the results showed its maximum value. The reason of maximizing this difference was the over-estimation of the code regulation in the same range of period values. This difference increased in the low period ratios (about 0.2 to 0.4) when the height of the base frame increased. As an example, in the period ratio of 0.3, the difference between the analytical and regulation results, when the base frame had 20 stories, approximately reached to 2 times

more than the case of the base frame with 10 stories. In the period ratio of 1, with increasing height of the base frame, this difference did not have a certain trend. For period ratios, which was more than 1, the difference of the results for different frames were approximately consistent. Considering the positive difference between the results of the analysis and the regulations of the Standard 2800 in Fig. 6, the SRSS method, (proposed by the Standard 2800 (ASCE7-16)), provided an over-estimate of the NSG in comparison with the results of the analysis.

### 6.2 Analytical Results of Regular Frames Adjacent to Irregular Frames

Regular and irregular frames were adjacent to each other according to the arrangement shown in Table 1 and the average angle of separation gap of the dynamic time history analysis under 20 records was compared with the results of the analysis of adjacent regular frames and the effects of irregularity of lateral stiffness was studied, as well.

Figure 7 showed the diagram of the variation in the NSG of the regular frame in left side based on combining with other frames in some adjacent cases. In mentioned figure, the regular base frame was located on the left and the other frames were arranged in three-regular cases, including irregular frame with irregularity factor of 1.3 and 1.6 corresponding to groups 1, 2, and 5 of the Table 1 which were adjacent to it. Then, the variation of the NSG had been given in terms of the period ratio of the right-side frame to the left-side frame. The results showed that generally, increasing the difference in height between the adjacent frames and increasing the lateral stiffness irregularity in the first story of the right side frames, increased the gap angle between them. As an example in Fig. 7(a) with 8-story base frame, the average of this increment, in combination of regular and irregular frames with an irregularity factor of 1.3 and 1.6, was respectively 1.20 and 1.57 times more than the combination of regular frames without

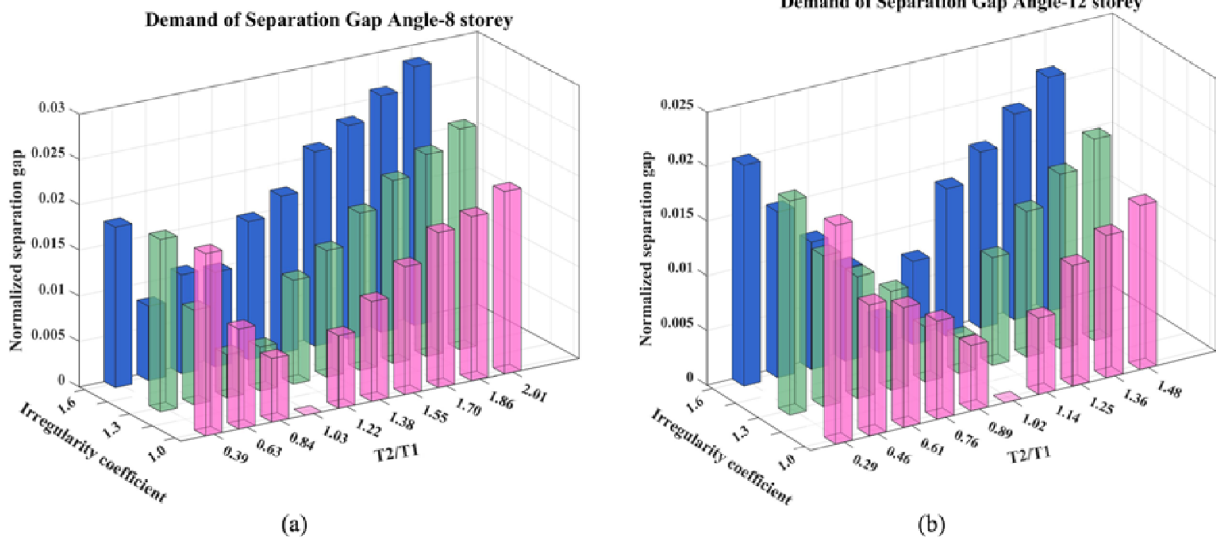


Fig. 7. Demand of NSG for Regular Frame (left side) in Combination with Irregular Frames (right side): (a) 8-Story Base Frame, (b) 12-Story Base Frame

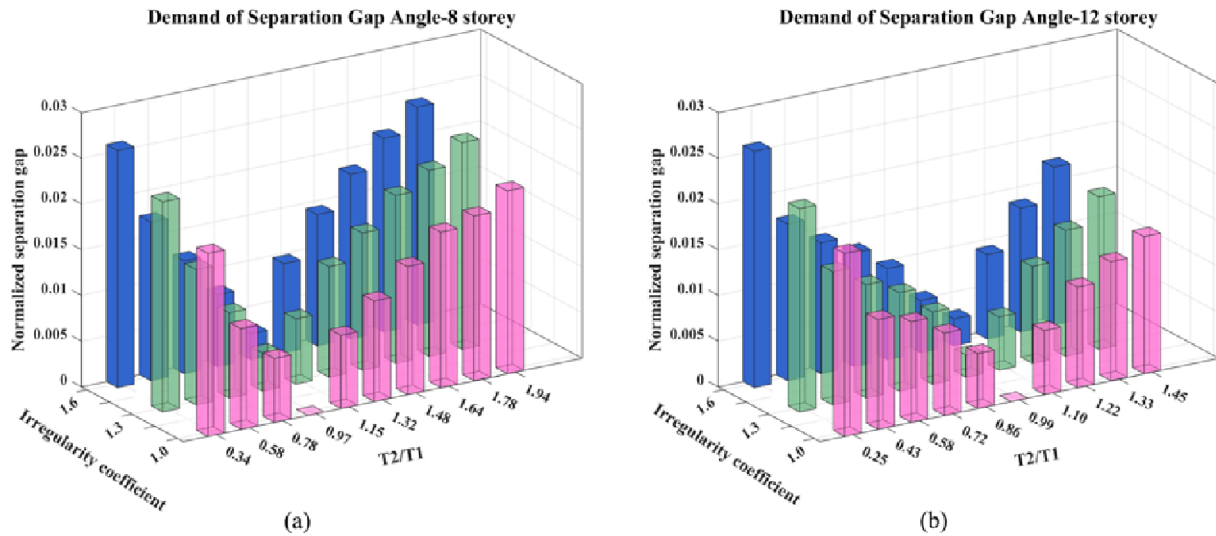


Fig. 8. Demand of NSG for Irregular Frame (left side) in Combination with Regular Frames (right side): (a) 8-Story Base Frame, (b) 12-Story Base Frame

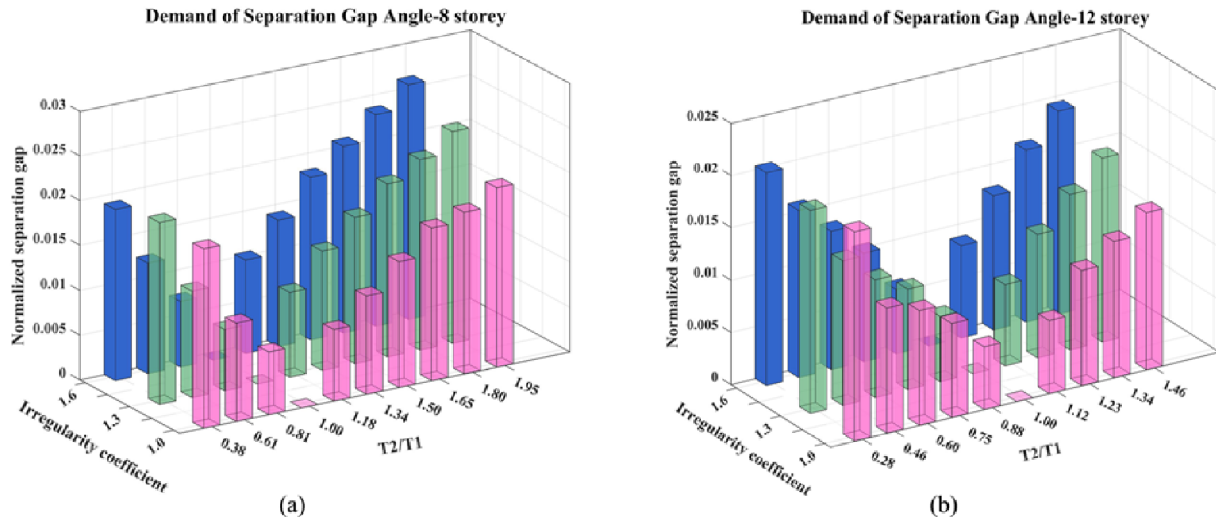


Fig. 9. Demand of NSG for Irregular Frame (left side) in Combination with Irregular Frames (right side): (a) 8-Story Base Frame, (b) 12-Story Base Frame

considering the adjacent state of the frames, which had equal number of stories. Therefore, if the lateral stiffness of the first story reduced by 53%, the NSG demand would increase by 20%. Whereas with a 74% reduction in lateral stiffness, the increase in NSG approached about 1.30 times more than previous state which represented nonlinear variation between the lateral stiffness of the first story and the NSG.

Figure 8 showed the diagram of the variation in the NSG of the irregular frame on left side based on combining with other frames presented in some adjacent cases. In mentioned figure, the base frame, in three regular and irregular cases with irregularity factors of 1.3 and 1.6, was on the left side and other regular frames corresponding to groups 1, 3 and 6 of Table 1, which were adjacent to it. Then, the variations in the NSG had been presented in terms of the period ratio of the two frames. The purpose of the recent evaluation compared with the similar

previous cases of (Efraimiadou et al., 2013b) and (Vaseghi and Jalali, 2013) was considering the effects of variation for the earthquake records, which was equivalent of moving on the layout of adjacent frames, and would lead to a change in the parameter, which was considered to be investigated. As an example in Fig. 8(a), in a 8-story base frame, the average of this increase, based on combinations of regular and irregular frames and irregularity factors of 1.3 and 1.6, was respectively 1.13 and 1.22 times more than the combination of regular frames without considering the adjacent cases of the frames with similar number of stories. In other words, a decrease of 53 and 74% in the lateral stiffness of first story would result in an increase of 13 and 22% in the NSG. Similar to the above results, the irregularity led to a significant NSG based on the combination of two irregular and regular adjacent frames with equal number of stories, and this demand increased with increasing irregularity rate.

The diagram of the variations of the NSG of the irregular frame in left side based on combination with the other irregular frames in some adjacent cases was shown in Fig. 9. In mentioned figure, the base frames were arranged in three regular and irregular cases, with irregularity factors of 1.3 and 1.6 on the left respectively corresponding to the mentioned cases. Other frames were arranged in three regular and irregular cases with irregularity factors of 1.3 and 1.6, in accordance with groups 1, 4 and 7 of Table 1 adjacent to it. As an example in Fig. 9(a) in a 8-story base frame, the average of this increase based on combinations with irregular frame and irregularity factors of 1.3 and 1.6 was, respectively, 1.18 and 1.31 times more than the combination of the regular frames without considering the adjacent state of the frames with equal number of stories. Thus, a decrease of 53 and 74% in lateral stiffness of the first story based on the combination of two irregular frames would result in an increase of 18 and 31% in the NSG, respectively. It should be noted that in two irregular frames with the same irregularity value and equal stories, the value of the NSG obtained from the analysis was zero, similar to the two regular frames with equal number of stories.

### 6.3 Summarizing Results of the Effect of Lateral Stiffness Irregularity on Demand of the Separation Gap

Figure 10 showed the conclusion of the results of Section 6.2 in a three-dimensional spot graph. The shell elements drawn in this figure is an interpolating of the results of the analysis, which is represented as point elements. In the diagrams of this figure, the horizontal axes represented the period ratio of structures in range of tall to short and the different values of the irregularity factors. The vertical axis represented the demand for NSG.

In Fig. 10(a), the amount of the demand of NSG had been given for the period ratio of the irregular and taller structure to the regular and shorter structure based on different values of irregularity factors. It could be seen that generally, by increasing the irregularity of lateral stiffness, the demand amount of the NSG increased. This increase was obvious, especially in higher period ratios as in the combination of 20IH(1.6).2RL with period ratio of 5.82; the amount of NSG demand reached the maximum value of 0.044. It should be noted that H indicated taller frame and L indicated shorter frame.

Figure 10(b) showed the demand amount of NSG for the period ratio of the regular and taller structure to the irregular and shorter structure based on different values of irregularity factors. The increase in demand of NSG with increasing in lateral irregularities, had no certain trend especially in low period ratio. Nevertheless, as shown in Fig. 10(a), this increase was evident in higher period ratios, based on the combination of 20RH.2IL(1.6) with the period ratio of 4.62; the demand amount of NSG reached the maximum value of 0.032.

The demand of NSG for the period ratio of the irregular and taller structure to the irregular and shorter structure in terms of various irregularity factors was shown in Fig. 10(c). This increase in the demand of NSG by increasing the irregularity factors at low period ratios was not clear. Nevertheless, like in the afore-

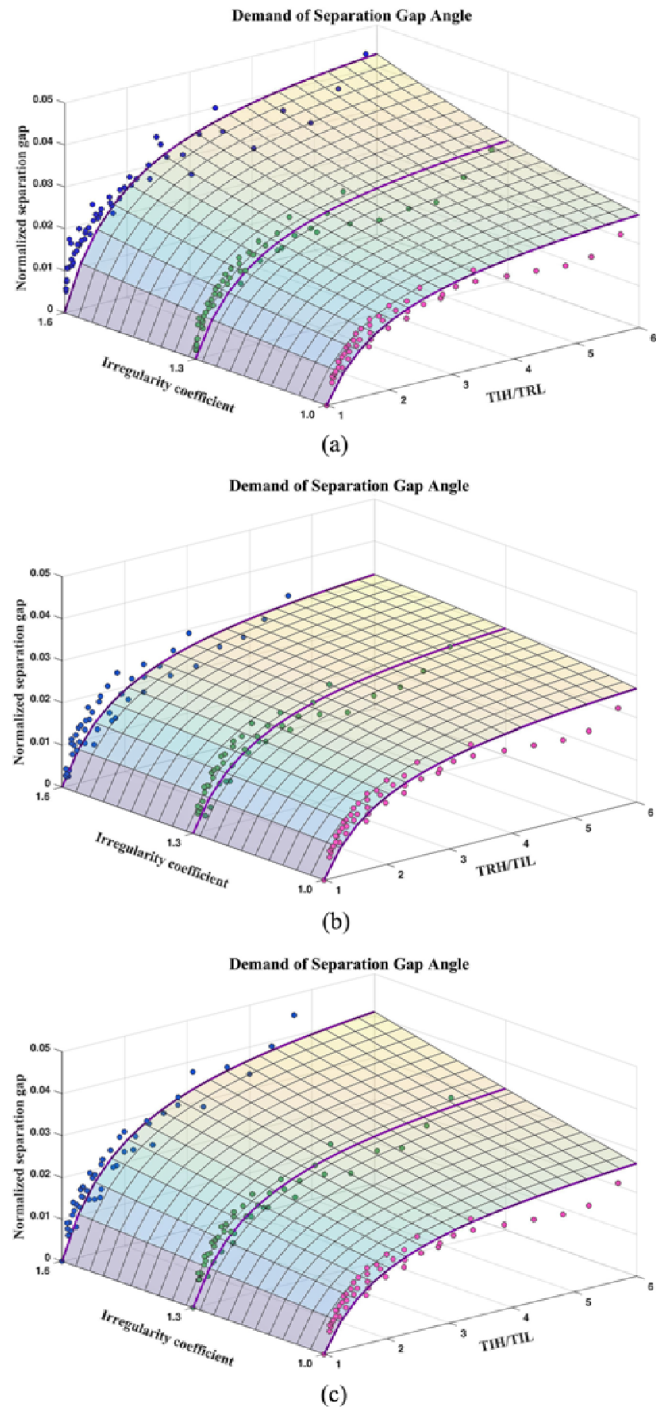


Fig. 10. Variation in NSG with the Variation in the Parameter of Irregularity of Lateral Stiffness: (a) TIH/TRL, (b) TRH/TIL, (c) TIH/TIL

mentioned case, this increase was evident in higher-period ratios, So that, the demand amount of NSG reached the maximum value of 0.045 in the combination of 20IH(1.6).2IL(1.6) with period ratio of 4.71. In general, Figs. 10(a) and 10(c) had the same values and trends in terms of the variation in the demand of NSG as compared to Fig. 10(b).

Table 3 showed that the variation in the demand of NSG had been shown based on 45 adjacent cases of each of the

**Table 3.** Variation in the Demand of NSG in 45 Adjacent Cases of Each Combination Relative to the Base Combination\*RH.\*RL

Adjacent combination	Percentage of affected cases	Average coefficient of increase	Maximum coefficient of increase
*IH(1.3).*RL	100%	1.28	1.51
*IH(1.6).*RL	100%	1.66	2.47
*RH.*IL(1.3)	53%	1.10	1.26
*RH.*IL(1.6)	62%	1.16	1.41
*IH(1.3).*IL(1.3)	91%	1.17	1.49
*IH(1.6).*IL(1.6)	93%	1.35	1.97

combinations relative to the base combination. It was necessary to explain that, the priority and delay on the arrangement of the layouts of the frames by choosing the maximum NSG of similar adjacencies and the adjacent state of the frames with equal number of stories had been ignored. On the other word, the maximum NSG had been selected from the analysis of two combinations of 4RH.2RL and 2RL.4RH. For more example, in the case of taller and irregular frames by an irregularity factor of 1.3 in the vicinity of shorter and regular frames were located in 45 cases (\*IH(1.3).\*RL); so that in all the cases, the NSG demand was increased relative to the adjacent case of the regular frame (\*RH.\*RL) and the average coefficient of this increase for all conditions was 28%. In addition, the maximum coefficient of this increase among the various combinations was 51% and it belonged to the combination 18IH.16RL. Therefore, the following table showed that the irregularity of lateral stiffness in the first story led to an increase in the NSG and this demand increased with increase in irregularity factor. In the irregular and taller frame combinations adjacent to the regular and shorter frame (\*IH.\*RL), the average and maximum coefficients of this increase in the demand of NSG were greater than the values of two irregular adjacent frame combinations (\*IH.\*IL). Also, the values of these coefficients in the recent case (\*IH.\*IL) were higher than the regular and taller frame combinations adjacent to the shorter and irregular frame (\*RH.\*IL).

If both adjacent regular or irregular frames had the same height for the first story, the value of the NSG of the analysis would be zero. However, if regular and irregular frames with equal number of stories adjacent to each other, the numerical NSG would be significant. Table 4 showed the variation of NSG at the highest collision level for regular and irregular frames with equal stories. By increasing the height of the collision zone and reducing lateral stiffness irregularity in the first story, the amount of NSG would decrease, in such a way that the maximum NSG occurred between the two 2-story regular and irregular frames at the lowest collision level. By increasing lateral stiffness irregularity on the first story, the amount of this demand increased so that, the average of this increase in regular and irregular frames with an irregularity factor of 1.6 and the same number of stories was 2.3 times more than the corresponding cases of irregular frames with an irregularity factor of 1.3.

**Table 4.** The Demand of NSG at the Highest Collision Level of Regular and Irregular Frame with Equal Number of Stories

Adjacent combination	NSG	Adjacent combination	NSG
2IH(1.3).2RL	0.0095	2IH(1.6).2RL	0.0191
4IH(1.3).4RL	0.0080	4IH(1.6).4RL	0.0172
6IH(1.3).6RL	0.0068	6IH(1.6).6RL	0.0161
8IH(1.3).8RL	0.0048	8IH(1.6).8RL	0.0104
10IH(1.3).10RL	0.0046	10IH(1.6).10RL	0.0104
12IH(1.3).12RL	0.0033	12IH(1.6).12RL	0.0076
14IH(1.3).14RL	0.0029	14IH(1.6).14RL	0.0072
16IH(1.3).16RL	0.0021	16IH(1.6).16RL	0.0050
18IH(1.3).18RL	0.0022	18IH(1.6).18RL	0.0055
20IH(1.3).20RL	0.0023	20IH(1.6).20RL	0.0056

Considering analyses results, the effect of parameters such as period and collision heights, story height and the first story height were studied and Eq. (12) was suggested to calculate the demand of NSG by selecting the appropriate objective function by nonlinear regressions, minimizing the average percentage error between analytical and estimated values. Eq. (12) consisted of three distinct sections. The first term was a combination of the period of structures, expressed the dynamic properties of adjacent structures. The second term represented the number of adjacent stories for the two structures and the third expression indicated the effects of lateral stiffness irregularity in the first story on the demand of NSG. As observed, the effects of irregularity in the first story had the nonlinear relation with demand of NSG. In accordance with the results of section 6.3, a higher power was proposed for its related parameter in Eq. (12) because of the greater effect of lateral stiffness in the first floor of the taller frame.

$$\alpha = 0.025 \left(1 - \frac{T_L}{T_H}\right) \left(\frac{H_L}{h_0}\right)^{0.15} \left(\frac{h_L^*}{h_0}\right)^{0.2} \left(\frac{h_H^*}{h_0}\right) \quad (12)$$

Where  $\alpha$  was the demand of NSG and  $T_H, T_L$  were the period of taller and shorter frames, respectively.  $H_L$  was the collision height (height of shorter frame),  $h_0$  was the height of stories for the shorter frame, and  $h_H^*, h_L^*$  were the first story height for the taller and shorter frames, respectively. The standard deviation of the obtained results of the analysis and the proposed values of the Eq. (12) was 71% of their average absolute error.

## 7. Validation of Proposed Relation

To validate the proposed relation, the demand of NSG obtained from the DDC method based on 15 various adjacent combinations of the studied regular frame was compared to the proposed Eq. (12) in Table 5. In this table, the lateral displacements  $u_1$  and  $u_2$  were obtained based on the average of structural analysis results under the 20 records at the highest collision level. In addition, the critical damping, in the calculation of the correlation coefficient was considered 0.05. The results showed a negligible and logical difference between the values of the NSG of the proposed

**Table 5.** Validation of the Demand of NSG Obtained from the Proposed Relation

Adjacent combination ( $i, j$ )	$u_1$ (cm)	$u_2$ (cm)	$T_1$ ( $T_L$ ) (sec)	$T_2$ ( $T_H$ ) (sec)	$H_L$ (cm)	Separation gap angle (DDC method)	Separation gap angle Eq. (12)	Ratio of DDC method to Eq. (12)
4,10	18.06	16.00	0.58	1.15	1,400	0.0171	0.0153	1.11
4,12	18.06	15.00	0.58	1.32	1,400	0.0167	0.0173	0.97
6,12	19.06	21.68	0.78	1.32	2,100	0.0135	0.0134	1.01
4,14	18.06	17.74	0.58	1.48	1,400	0.0180	0.0187	0.96
6,14	19.06	24.60	0.78	1.48	2,100	0.0147	0.0155	0.95
8,14	25.62	29.30	0.97	1.48	2,800	0.0135	0.0118	1.14
2,16	14.48	8.18	0.34	1.64	700	0.0237	0.0219	1.08
6,16	19.06	27.08	0.78	1.64	2,100	0.0157	0.0171	0.92
8,16	25.62	33.00	1.15	1.64	3,500	0.0147	0.0139	1.06
4,18	18.06	20.14	0.58	1.78	1,400	0.0193	0.0207	0.93
8,18	25.62	36.90	0.97	1.78	2,800	0.0159	0.0155	1.03
10,18	34.00	41.84	1.32	1.78	4,200	0.0150	0.0125	1.20
6,20	19.06	34.45	0.97	1.94	2,800	0.0187	0.0196	0.95
8,20	25.62	42.27	1.15	1.94	3,500	0.0175	0.0170	1.03
10,20	34.00	47.50	1.48	1.94	4,900	0.0164	0.0144	1.14

relation compared to the DDC method, so that the difference between the values of the mentioned relations for the combinations studied was less than 20%.

## 8. Conclusions

Demand of NSG was estimated in this study, based on 700 combinations of regular and irregular adjacent MRFs at the highest collision level. The results of carried out analyses under 20 components perpendicular to the fault of near-fault earthquakes were:

1. In some adjacent cases of examined regular frames, the results of the demand of NSG obtained from the analysis in the combination up to the 8-story regular frames were higher than the values of Standard 2800, which represented the under-estimation of the NSG of the regulation.
2. The NSG obtained from Standard 2800 (ASCE7-16) based on the combination of frames with a height of more than eight stories was greater than the analytical values. This difference, in particular, on frames with equal period reached to their maximum value and expressed a conservative estimate of the regulation NSG in the range of vicinities of the frames with equal period.
3. By increasing the irregularity of the lateral stiffness, with the variation in the first story height of the frames, the NSG between adjacent frames increased in 84% of the adjacent combinations. The average coefficient of this increase from the combination of regular and irregular frames with irregularity factors of 1.3 and 1.6 was 1.18 and 1.39 times the regular frame combinations, respectively.
4. Among the different combinations for regular and irregular adjacent frames, when taller structure has lateral stiffness irregularity in the first story, the average coefficient of the

NSG increment relative to the regular adjacent combination was more than the other cases. Thus, the average coefficient of this increase for irregular frame combinations with irregularity factors of 1.3 and 1.6 was 1.28 and 1.66, respectively.

5. Irregularity led to a significant NSG increment in combination of two regular and irregular adjacent frames with equal number of stories and with increase in irregularity. This demand increased, so that the average of this increase in irregular frames by an irregularity factor of 1.6 was 2.3 times more than the irregular frames by an irregular factor of 1.3.
7. A relation was proposed to estimate the demand of the NSG of adjacent frames by considering the effects of lateral stiffness irregularities of in the lower story and the validity of the relation was evaluated through numerical analysis.

## Acknowledgements

Not Applicable

## ORCID

Mostafa Khatami <https://orcid.org/0000-0003-0104-645X>  
 Mohsen Gerami <https://orcid.org/0000-0002-4113-932X>  
 Ali Kheyroddin <https://orcid.org/0000-0001-7802-2013>  
 Navid Siahpolo <https://orcid.org/0000-0002-7813-9008>

## References

ASCE/SEI 7-16 (2016) Minimum design loads for buildings and other structures. Standard ASCE/SEI 7-16, American Society of Civil

- Engineers, Reston, VA, USA
- Baker JW (2007) Quantitative classification of near-fault ground motions using wavelet analysis. *Bulletin of the Seismological Society of America* 97(5):1486-1501, DOI: [10.1785/0120060255](https://doi.org/10.1785/0120060255)
- Efraimiadou S, Hatzigeorgiou GD, Beskos DE (2013a) Structural pounding between adjacent buildings subjected to strong ground motions. PartI: The effect of different structures arrangement. *Earthquake Engineering & Structural Dynamics* 42:1509-1528, DOI: [10.1002/eqe.2285](https://doi.org/10.1002/eqe.2285)
- Efraimiadou S, Hatzigeorgiou GD, Beskos DE (2013b) Structural pounding between adjacent buildings subjected to strong ground motions. PartII: The effect of multiple earthquakes. *Earthquake Engineering & Structural Dynamics* 42:1529-1545, DOI: [10.1002/eqe.2284](https://doi.org/10.1002/eqe.2284)
- ETABS (2015) Analysis reference manual, version 15.2.2. Computers and Structures Inc., Berkeley, CA, USA
- Favvata MJ (2017) Minimum required separation gap for adjacent RC frames with potential inter-story seismic pounding. *Engineering Structures* 152:643-659, DOI: [10.1016/j.engstruct.2017.09.025](https://doi.org/10.1016/j.engstruct.2017.09.025)
- Hao H (2015) Analysis of seismic pounding between adjacent buildings. *Australian Journal of Structural Engineering* 16(3):208-225, DOI: [10.1080/13287982.2015.1092684](https://doi.org/10.1080/13287982.2015.1092684)
- INBC-No.6 (2014) Design loads for buildings. Iranian National Building Code No.6, Road, Housing and Urban Development Research Center, Iran
- INBC-No.10 (2014) Design and construction of steel structures. Iranian National Building Code No.10, Road, Housing and Urban Development Research Center, Iran
- Jankowski R (2005) Non-linear viscoelastic modelling of earthquake-induced structural pounding. *Earthquake Engineering & Structural Dynamics* 34:595-611, DOI: [10.1002/eqe.434](https://doi.org/10.1002/eqe.434)
- Karayannis C, Favvata MJ (2005) Earthquake-induced interaction between adjacent reinforced concrete structures with non-equal heights. *Earthquake Engineering & Structural Dynamics* 34(1):1-20, DOI: [10.1002/eqe.398](https://doi.org/10.1002/eqe.398)
- Khatami M, Gerami M, Kheyroddin A, Siahpolo N (2019) The effect of the mainshock–aftershock on the estimation of the separation gap of regular and irregular adjacent structures with the soft story. *Journal of Earthquake and Tsunami*, DOI: [10.1142/S1793431120500086](https://doi.org/10.1142/S1793431120500086)
- Kheyroddin A, Kioumars M, Kioumars B, Farai A (2018) Effect of lateral structural systems of adjacent buildings on pounding force. *Engineering and Structures* 14(3):229-239, DOI: [10.12989/eas.2018.14.3.229](https://doi.org/10.12989/eas.2018.14.3.229)
- López-Almansa F, Kharazian A (2018) New formulation for estimating the damping parameter of the Kelvin-Voigt model for seismic pounding simulation. *Engineering Structures* 175:284-295, DOI: [10.1016/j.engstruct.2018.08.024](https://doi.org/10.1016/j.engstruct.2018.08.024)
- McKenna F, Fenves G (2007) Open System for Earthquake Engineering Simulation. University of California, Berkeley, CA, USA
- Naderpour H, Khatami SM, Barros RC (2017) Prediction of critical distance between two MDOF systems subjected to seismic excitation in terms of artificial neural networks. *Periodica Polytechnica Civil Engineering* 9618, DOI: [10.3311/PPci.9618](https://doi.org/10.3311/PPci.9618)
- PEER (2018) Pacific earthquake engineering research center. Retrieved March 20, 2018, <https://peer.berkeley.edu/peer-strong-ground-motion-databases>
- SeismoSignal (2016) A computer program for signal processing of strong-motion data, Version 5.1.2. Seismosoft
- Shehata E, Raheem A (2014) Mitigation measures for earthquake induced pounding effects on seismic performance of adjacent buildings. *Bulletin of Earthquake Engineering* 12:1705-1724, DOI: [10.1007/s10518-014-9592-2](https://doi.org/10.1007/s10518-014-9592-2)
- Shrestha B (2013) Effects of separation distance and nonlinearity on pounding response of adjacent structures. *International Journal of Civil and Structural Engineering* 3(3):603-612, DOI: [10.6088/ijcser.201203013055](https://doi.org/10.6088/ijcser.201203013055)
- Standard No.2800 (2014) Iranian code of practice for seismic resistant design of buildings, 4th edition. Road, Housing and Urban Development Research Center, BHRC Publication, Iran
- Takabatake H, Yasui M, Nakagawa Y, Kishida A (2014) Relaxation method for pounding action between adjacent buildings at expansion joint. *Earthquake Engineering & Structural Dynamics* 43:1381-1400, DOI: [10.1002/eqe.2402](https://doi.org/10.1002/eqe.2402)
- Vaseghi J, Jalali SG (2013) Park-Ang damage index for adjacent steel frames under pounding. *Journal of the Croatian Association of Civil Engineers* 12:1065-1077, DOI: [10.14256/JCE.921.2013](https://doi.org/10.14256/JCE.921.2013)